

Transition from Stick-Slip to Continuous Sliding in Atomic Friction: Entering a New Regime of Ultralow Friction

A. Socoliuc, R. Bennewitz,* E. Gnecco, and E. Meyer

Institute of Physics, University of Basel, Klingelbergstrasse 82, CH-4056 Basel, Switzerland

(Received 10 December 2003; published 1 April 2004)

A transition from stick-slip to continuous sliding is observed for atomically modulated friction by means of a friction force microscope. When the stick-slip instabilities cease to exist, a new regime of ultralow friction is encountered. The transition is described in the framework of the Tomlinson model using a parameter η which relates the strength of the lateral atomic surface potential and the stiffness of the contact under study. Experimentally, this parameter can be tuned by varying the normal load on the contact. We compare our results to a recently discussed concept called superlubricity.

DOI: 10.1103/PhysRevLett.92.134301

PACS numbers: 46.55.+d, 68.37.Ps

The understanding and control of frictional properties of matter at the nanometer scale remains a great challenge for a wide spectrum of sciences, ranging from engineering studies of micromachine lubrication to atomistic simulations of nanometer-scale systems. Measurements of lateral forces which reveal the atomic structure of the materials under study can contribute to our understanding of mechanical dissipation, as atomic friction can be seen as an elementary process of the dissipation. The first observation of atomic friction processes was reported by Mate *et al.* for a tungsten tip sliding over graphite [1]. By means of a friction force microscope they found a sawtoothlike modulation of the lateral force with the periodicity of the graphite's honeycomb structure. An accurate description of the experiment and the underlying mechanisms was given by Tománek *et al.*, who based their description on the Tomlinson model for molecular friction [2]. Basically, the tip is dragged over the periodic potential defined by the atomic structure of the surface and the contact. The lateral force is measured by means of a cantilever spring holding the tip. The tip sticks to a certain surface position until the force exerted by the moving support of the spring is high enough to activate a slip of the tip to the next atomic position. This stick-slip behavior shows up as the sawtoothlike modulation of the lateral force. However, there is a condition for observing the stick-slip instability: The elastic constant of the pulling spring must be smaller than the curvature of the surface potential corrugation. Otherwise, the hard spring would move the contact over the surface in a continuous sliding. In this Letter we report on the first experimental observation of the transition from stick-slip to continuous sliding in atomic friction. The latter is inherently linked to a regime of ultralow dissipation.

Our measurements were realized with a homebuilt friction force microscope operated at room temperature under ultrahigh vacuum conditions [3]. Silicon cantilevers with a spring constant of $k_N = 0.05$ N/m for normal bending and $k_T = 29$ N/m for torsion were used. The radius of curvature of the tip was nominally below

15 nm (Nanosensors from Nanoworld). The feedback loop controlling the tip-sample distance was operated very slowly, in order to avoid any influence of the feedback on the measurement of the lateral forces. The experiments were performed on NaCl single crystals cleaved in UHV and heated at 150 °C to remove charges produced in the cleaving process. The normal and lateral forces acting on the tip were calibrated according to the procedures given in Ref. [4].

Figures 1(a)–1(c) show the lateral force F_L recorded with three different externally applied normal loads F_N . Note that the total normal force between tip and surface is the sum of the externally applied load and the attractive force between tip and sample. The latter has been determined to be 0.7 nN by measuring the force required to pull the tip out of contact. The scan velocity was $v = 3$ nm/s.

For $F_N = 4.7$ nN the lateral force reveals two opposite sawtooth profiles when scanning forwards and backwards [Fig. 1(a)]. The sawtooth modulation has the periodicity of the crystal lattice along the (100) direction and is characteristic for the stick-slip process. The area enclosed in this hysteresis loop is the energy dissipated in one cycle. When the externally applied load is lowered to 3.3 nN the dissipated energy decreases, while the amplitude of the sawtooth modulation stays constant resulting in an overlap of the curves for the forward and the backward scan. In fact, the lateral force changes its sign in the slip event [Fig. 1(b)]. While the moving spring is pulling on the contact before the slip, the contact is pulling on the spring after it has slipped to the next atomic position and, thereby, has surpassed the moving support of the spring. A similar load dependence of the stick-slip behavior has been observed on the layered materials graphite and MoS₂ and normal loads of higher orders of magnitude [1,5].

A completely different picture is found when the load is further reduced. For normal loads below a certain threshold, the hysteresis loop and with it the dissipation disappears within the sensitivity of the current experiment

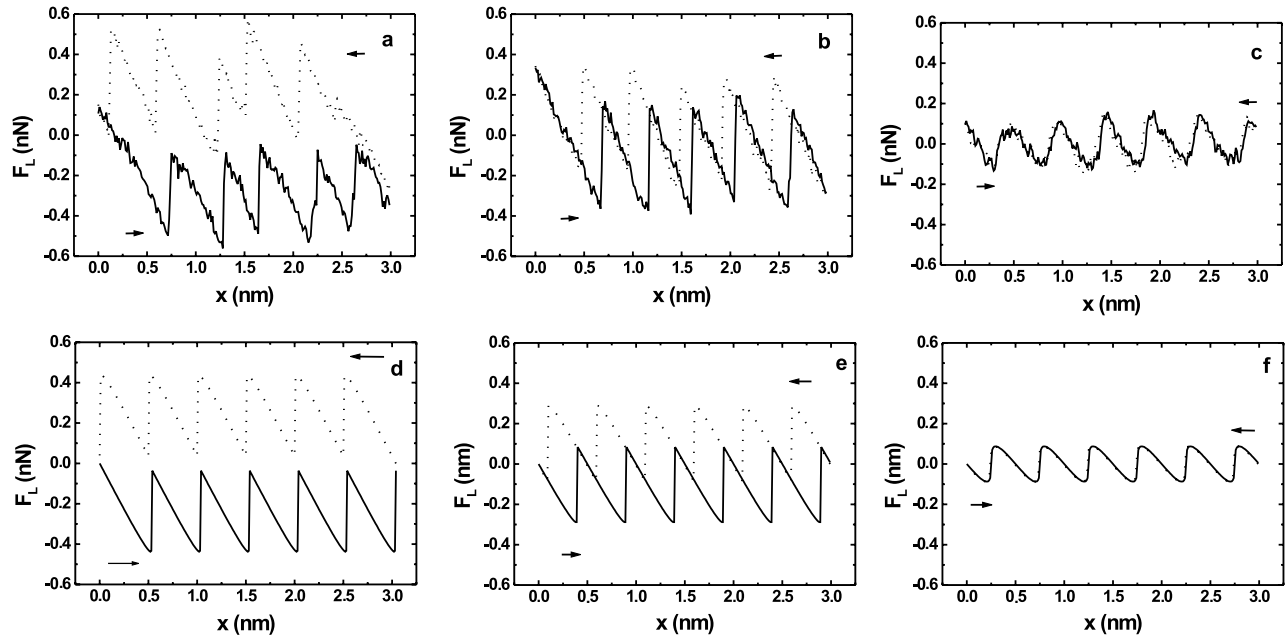


FIG. 1. (a)–(c) Measurements of the lateral force acting on the tip sliding forward and backward in (100) direction over the NaCl(001) surface. The lines are typical cross sections through a two-dimensional scan along the strongest force amplitude. The externally applied load was (a) $F_N = 4.7$ nN, (b) $F_N = 3.3$ nN, and (c) $F_N = -0.47$ nN. (d)–(f) Corresponding numerical results from the Tomlinson model for (d) $\eta = 5$, (e) $\eta = 3$, and (f) $\eta = 1$. The stiffness was chosen as $k = 1$ N/m and the lattice constant as $a = 0.5$ nm. Note that for values of $\eta \leq 1$ the hysteresis loop enclosed between the forward and the backward scan vanishes; i.e., there is no more dissipation within this model.

[Fig. 1(c)]. Simultaneously, the sawtooth modulation of the lateral force is transformed into a continuous modulation of perfect match between forward and backward scan, still showing the atomic periodicity of the surface lattice. Similar features were revealed with other tips on different spots of the crystal surface. The tips were never crashed or operated at high loads. In all cases the quality of the signal-to-noise ratio is reduced after prolonged scanning, making it difficult to recognize the transition from the stick-slip regime to continuous sliding.

The observed transition can be explained in a classical one-dimensional Tomlinson-type model. We assume that the tip is dragged over a sinusoidal potential with amplitude E_0 and periodicity a . The pulling spring which is extended between the position of the tip x_{tip} and the position of the moving support x_s has an effective spring constant k . Note that in the experiment this spring constant is not just that of the torsional bending of the cantilever k_T but combines the stiffness of the cantilever and the lateral stiffness of the contact. In the model, the tip always resides in a minimum of the effective potential

$$V = -\frac{E_0}{2} \cos\left(2\pi \frac{x_{\text{tip}}}{a}\right) + \frac{1}{2} k(x_{\text{tip}} - x_s)^2. \quad (1)$$

The movement of the tip from one minimum to the next can be continuous or jumping, depending on the relation between corrugation E_0 and elastic energy which can be described by a parameter

$$\eta = \frac{2\pi^2 E_0}{ka^2}. \quad (2)$$

When $\eta < 1$ the movement is continuous and no dissipation occurs; when $\eta > 1$ the stick-slip behavior is found. Numerical results for three different values of η are presented in Figs. 1(d)–1(f).

Experimentally, the dissipation or, correspondingly, the mean friction force decreases with decreasing normal load and reaches zero before the sliding tip jumps out of contact. In the model, the dissipation decreases for decreasing η and is zero for all values $\eta \leq 1$. These two dependencies are compared in Fig. 2. The similarity of the two curves brings us to the question of how far the parameter η of the Tomlinson model is accessible to the experiment via variation of the normal load. In order to answer the question, we determine all parameters of the Tomlinson model by a detailed analysis of the experimental data.

The corrugation of the surface potential E_0 is linearly related to the maximum lateral force F_L^{max} . This can be found by analyzing the conditions for the position of the tip ($\partial V / \partial x_{\text{tip}} = 0$). With $F_L = k(x_{\text{tip}} - x_s)$, it follows that

$$F_L = -\frac{\pi E_0}{a} \sin\left(2\pi \frac{x_{\text{tip}}}{a}\right). \quad (3)$$

The maximum of the absolute value of the force F_L^{max} is found at $x_{\text{tip}} = a/4$, and we obtain

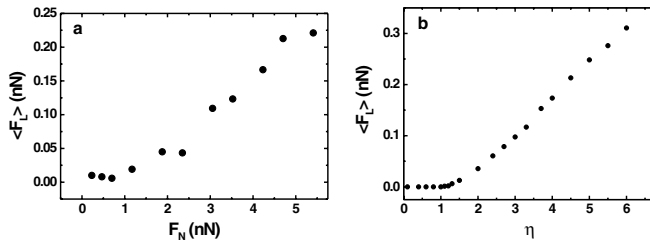


FIG. 2. (a) Mean lateral force versus normal load. The experimentally determined adhesion has been added to the externally applied load. The data points represent the average over a two-dimensional scan of $3 \times 3 \text{ nm}^2$. (b) Numerical evaluation of the mean lateral force as a function of the parameter η in the one-dimensional Tomlinson model. Quantitative difference between experimentally and numerically obtained forces can result from the two-dimensional averaging in the case of experimental results. The numerical results have been calculated for lines with maximal corrugation, like those presented in Fig. 1.

$$E_0 = \frac{aF_L^{\max}}{\pi}. \quad (4)$$

The load dependence of the potential corrugation E_0 is obtained from the maxima of curves like the ones in Figs. 1(a)–1(c) and is shown in Fig. 3(a). A second important quantity that can be extracted from the data is the slope k_{exp} of the lateral force versus displacement at the beginning of each stick phase [Fig. 3(b)]. For large values of η , i.e., for a strong potential E_0 or weak stiffness k , this slope directly reveals k [6]. For η approaching 1, however, the relation has to be corrected [7], and already knowing E_0 we can determine η as

$$\eta = \frac{2\pi F_L^{\max}}{k_{\text{exp}} a} - 1. \quad (5)$$

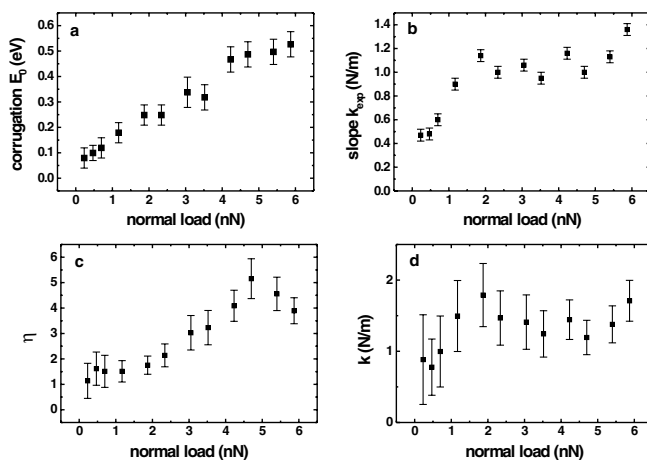


FIG. 3. (a) Energy corrugation E_0 , (b) slope k_{exp} of the lateral force versus distance in the sticking part, (c) parameter η , and (d) effective lateral stiffness k of the contact, as a function of the normal load F_N acting on the tip.

Figure 3(c) shows how, within the errors, η indeed approaches 1 for those normal loads with a vanishing stick-slip process. Finally, we can calculate the effective lateral stiffness

$$k = \frac{\eta + 1}{\eta} k_{\text{exp}}, \quad (6)$$

which is plotted in Fig. 3(d). Comparing the results we find that the corrugation of the surface potential E_0 increases much stronger with load than the effective stiffness k , which is nearly constant. This finding explains why a variation of the normal load changes the relation η between the two quantities and, therewith, allows us to study the transition from stick-slip to continuous sliding.

The increase of the corrugation height of the potential with increasing normal load can be intuitively understood as an increase of the barrier height between adjacent atomic positions when the contacting atoms are pressed closer towards the surface lattice. For a different atomic system this effect has been confirmed in a first principles study [8]. The small variation of the effective stiffness with normal load is not as easy to understand. First let us note that the effective stiffness is of the order of 1 N/m, a range we have found in most of our atomic friction studies on different materials. The lateral stiffness of the force sensor is usually at least a factor of 50 higher. The cantilever and the deformable contact can be seen as springs in series. Therefore, the effective stiffness is clearly dominated by the contact which is a much weaker spring. For the occurrence of stick-slip processes in atomic friction, the stiffness of the cantilever-type force sensor does not play any significant role, as confirmed experimentally [9]. The reason for the constancy of the contact stiffness could be explained in a straightforward manner by assuming that the atomic structure of the contact does not change in this range of normal loads. In this case, the deformability of the structure at the tip apex and of the surface around the contact would not change significantly with load. If the size or the atomic structure of the contact would change with load, the scaling of the corrugation and the stiffness would depend strongly on the dimensionality and commensurability of the contact [10].

Frictionless sliding was discussed thoroughly by McClelland [11]. Negligible friction between two solid surfaces is predicted by both an independent oscillator model and the Frenkel-Kontorowa model, when the interfacial interactions are weak or the surfaces are incommensurate. A further support to this conclusion was given by two-dimensional numerical simulations. Vanishing friction on a silicon surface was observed by Hirano *et al.* with scanning tunneling microscopy [12]. This effect was called “superlubricity,” and it was related to the incommensurate contact between tip and surface. The underlying idea is that the contributions to the friction

force coming from the mismatched atoms in the contact area point in all directions and sum up to zero [13]. A corroboration of the idea has been recently reported by Dienwiebel *et al.*, who found that friction between graphite surfaces is significantly reduced when the surfaces are rotated out of the commensurate locking angle [14]. The state of ultralow friction demonstrated in this Letter is based on a similar concept. Negative and positive lateral forces sum up to a vanishing average force in the time average instead of the spatial average, provided there are no instabilities. In contrast to Hirano's model, no assumptions for a large contact size, hardness of the lattices, or commensurability have to be made.

We refrain from using the term superlubricity, since it suggests that the transition to zero friction can be compared to superfluidity or superconductivity. However, this is certainly not an effect of quantum mechanical coherence. Furthermore, we assume that the mean friction is not zero, although we cannot measure any lateral force with the current signal-to noise ratio. The movement of the tip must be heavily damped, as we do not observe any overshooting or jumps over two lattice constants under stick-slip conditions. Consequently, there must be some energy loss mechanism in the tip movement beyond the internal damping of the force sensor. There is no reason to assume that this energy mechanism disappears for $\eta \leq 1$. What disappears, however, are the instabilities which, under stick-slip conditions, give the dominant contribution to the observed dissipation.

It is important to note that a similar transition from stick-slip to continuous sliding has been observed in the manipulation of single Pb atoms by means of a scanning tunneling microscope [15]. In their study, Bartels *et al.* found a stick-slip process when the tip was moving relatively far from the Pb atom, while continuous sliding was observed with the tip in close proximity to the atom. The situation can be described in the same model as our experiment, but with the opposite tendencies. In the atom manipulation experiment, the surface corrugation felt by the Pb atoms is always the same. When the tip was approached, the effective spring constant of the coupling between tip and atoms became higher, and therefore the stick-slip disappeared.

In summary, we have experimentally demonstrated and theoretically described a state of ultralow dissipation in atomic friction which is connected to the absence of mechanical instabilities. These can be controlled by variation of the load on the contact which changes

the atomic corrugation felt by the contact more than its stiffness. The results demonstrate how friction can be controlled on the nanometer scale and how stiff contacts with a binding in the contact that causes a weak potential against lateral sliding can practically eliminate dissipation.

The authors are grateful to A. Baratoff for fruitful discussions. This work was supported by the Swiss National Science Foundation, the Kommission zur Förderung von Technologie und Innovation, and the National Center of Competence in Research on Nanoscale Science.

*Now at Physics Department, McGill University, Montreal, Canada.

Electronic address: roland.bennewitz@unibas.ch

- [1] C. Mate, G. McClelland, R. Erlandsson, and S. Chiang, *Phys. Rev. Lett.* **59**, 1942 (1987).
- [2] D. Tománek, W. Zhong, and H. Thomas, *Europhys. Lett.* **15**, 887 (1991).
- [3] L. Howald, E. Meyer, R. Lüthi, H. Haefke, R. Overney, H. Rudin, and H.-J. Güntherodt, *Appl. Phys. Lett.* **63**, 117 (1993).
- [4] E. Meyer, H. Hug, and R. Bennewitz, *Scanning Probe Microscopy* (Springer-Verlag, Berlin, 2003).
- [5] S. Fujisawa, E. Kishi, Y. Sugawara, and S. Morita, *Phys. Rev. B* **52**, 5302 (1995).
- [6] R. Carpick, D. Ogletree, and M. Salmeron, *Appl. Phys. Lett.* **70**, 1548 (1997).
- [7] E. Gnecco, R. Bennewitz, T. Gyalog, and E. Meyer, *J. Phys. Condens. Matter* **13**, R619 (2001).
- [8] W. Zhong and D. Tománek, *Phys. Rev. Lett.* **64**, 3054 (1990).
- [9] R. Bennewitz, T. Gyalog, M. Guggisberg, M. Bammerlin, E. Meyer, and H.-J. Güntherodt, *Phys. Rev. B* **60**, R11301 (1999).
- [10] M. Mueser (to be published).
- [11] G. McClelland, in *Adhesion and Friction*, edited by M. Grunze and H. Kreuzer (Springer-Verlag, Berlin, 1989), p. 1.
- [12] M. Hirano, K. Shinjo, R. Kaneko, and Y. Murata, *Phys. Rev. Lett.* **78**, 1448 (1997).
- [13] M. Hirano, *Wear* **254**, 932 (2003).
- [14] M. Dienwiebel, G. Verhoeven, N. Pradeep, J. Frenken, J. Heimberg, and H. Zandbergen, *Phys. Rev. Lett.* **92**, 126101 (2004).
- [15] L. Bartels, G. Meyer, and K.-H. Rieder, *Phys. Rev. Lett.* **79**, 697 (1997).